Algerian Journal of Engineering and Technology 02 (2020) 022–028

Algerian Journal of Engineering and Technology

Journal homepage: https://jetjournal.org/index.php/ajet

Original Article

Experimental study of exfoliation corrosion-induced mechanical properties degradation of Aluminum alloys: 2024-T3 and 5083-H22

Abdessamad Brahami[a,*], Jamel Fajoui[b], Benattou Bouchouicha[a]

[a] *Université Djilali Liabes, BP 89, Sidi Bel Abbes, 22000, Algeria*

[b] *Institut Universitaire de Technologie de Saint Nazaire, 58 rue Michel Ange - BP 420, Saint Nazaire, 44606, France.*

ARTICLE INFO

Article history:
Received 17 November 2019
Revised 17 December 2019
Accepted 4 February 2020

Keywords:
Aluminum alloys;
Mechanical properties;
Microstructure;
Exfoliation corrosion;
Precipitation,
SEM.

ABSTRACT

In the present paper, the impact of exfoliation corrosion (EFC) of 2024 and 5083 aluminum alloys on the residual mechanical properties was investigated. Tensile test had been carried out on pre-corroded specimens, exposed to laboratory accelerated exfoliation corrosion solution. The analysis suggests that exfoliation exposure leads to decrease the mechanical properties of all materials. The effects of the grain boundary character distribution and precipitates on corrosion are discussed on the basis of experimental observations by Scanning Electron Microscope SEM combined with Energy Dispersive Spectroscopy EDS analysis.

1. Introduction

Aluminum alloys occupy a very important place in the aeronautical, industrial and transport fields. Localized corrosion is a major cause of their failure. Among various kinds of localized corrosion that aluminum alloys undergo, exfoliation corrosion is an important form. EFC is thought to be a particular form of intergranular corrosion (IGC) that can occur on the surface of wrought aluminum alloys with an elongated grain structure [1]. During this corrosion process, internal stresses caused by voluminous corrosion products force layers of un-corroded metal away from the body of the material, giving rise to a layered appearance [2]. EFC can lead to metal failure by gradual disintegration and the presence of exfoliation corrosion reduces the toughness of the alloy and enhances the fatigue crack growth rate [3-7]. All of these will cause serious problems to structures and limit their lifetime. EFC has been studied since the 1950s, yet crucial phenomena remain unclear. Several papers suggested that the exfoliation corrosion results either from intergranular corrosion or alternatively from a stress corrosion mechanism. Experiments conducted by Robinson's group have shown a strong similarity between the mechanism of stress corrosion cracking (SCC) and EFC mechanism [1, 8-10]. However, exactly how this mechanism works in the case of EFC is still unknown. Though many efforts have been made to enhance the resistance of aluminum alloys to EFC, the lack of a quantification method and limited laboratory tests for EFC have slowed down the development of protection methods for EFC. So, we understand the interest to study the mechanisms of corrosion of AA2024 T3 and AA5083 H22 and then, see the influence of these mechanisms on the microstructure and on mechanical properties. These two lines of research on the corrosion of the two alloys constitute the objectives of this work. The present work is essentially based on two parts, on the one hand, mechanical and microstructural characterization of non-corroded specimens. Other hand, a chemical attack to provoke corrosion on the different samples and specimens of the different materials; After this chemical attack, all characterizations cited above were done again. Two alloys 2024 and 5083 has been studied by immersion in the EXCO solution according to ASTM G34-01[11].

* *Corresponding author.* Tel.: +213675894166
E-mail address: Abdessamad.brahami@univ-sba.dz

Peer review under responsibility of University of Echahid Hamma Lakhdar.
http://dx.doi.org/10.5281/zenodo.3924714

Macroscopic observations were illustrated to see the degree of severity of corrosion. Then, a detailed study of the microstructure by scanning electron microscope (SEM) and Energy Dispersive Spectroscopic (EDS) in order to be able to correlate the influence of the state of the microstructure on the corrosion behavior and on mechanical properties has been conducted.

2. Testing procedure

The materials studied in the present work are two grades of aluminium alloy, the 2024-T3 which belongs to the second group representing heat-treated or precipitation hardening alloys. The 5083-H22 that belongs to the first group representing strain hardening alloys. Table 1 gives the chemical composition of these alloys as determined by the EDS method.

Table 1 Typical chemical composition of the aluminum alloys (% weight)

	Element (%)								
Aluminum	**Si**	**Mg**	**Fe**	**Cu**	**Mn**	**Cr**	**Zn**	**Ti**	**Al**
2024-T3	0.06	1.57	0.17	4.45	0.56	0.1	0.16	0.15	BAL.
5083-H22	0.57	1.38	0.64	0.42	1.19	0.05	0.01	0.04	BAL

Monotonic tensile tests were performed on an INSTRON 8516 testing machine to determine the mechanical properties of the materials before and after the chemical attack. The tests were performed using standard rectangular tension specimens according to ASTM E8 [12] with a moving crosshead speed set at 2 mm/min, at room temperature and in air-laboratory. The dimensions of the specimen are given in Figure 1.

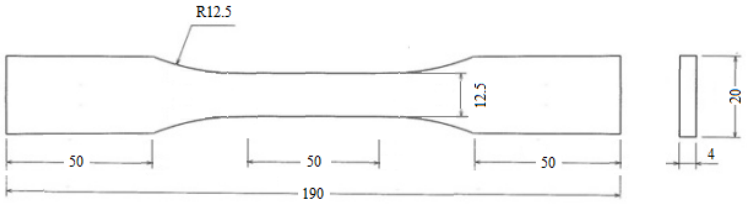

Fig. 1. Tensile test specimen

For microstructural observation, all samples were cut from different materials with a dimension of 10 by 10 mm. The samples were polished by 1400 abrasive paper. A qualitative analysis by Qunata 250 field emission scanning electron microscopy (FE-SEM) with an EDS in the backscattered mode was used to observe the evolution of the microstructure and to perform analysis in order to determine chemical composition for the materials and then identify the precipitates of each grade as well as its chemical composition. To evaluate the degradation of the mechanical properties of the material, specimens and samples were exposed to exfoliation corrosion according to the ASTM G34-01 specification. The corrosive solution consists of chemicals diluted in 1 l of distilled water. These were: sodium chloride (4.0 M NaCl, 3.5 wt%), potassium nitrate (0.5 M KNO3) and nitric acid (0.1 M HNO3, 70 wt%). The initial apparent pH of the solution was 0.4. The solution volume per exposure area was 17.5 ml/cm2 and the solution temperature was 25±3 °C. The specimens were immersed in the solution for 96 H for AA2024 and 72 H for AA5083. The next steps are respected to describe the procedure of this constant immersion test: Degrease the samples with an appropriate solvent. We used in this study: 945 ml of distilled water, 50 ml of nitric acid HNO3 solvent and 5ml hydrofluoric acid HF for degreasing. Then, use the attack solution in sufficient quantity to provide a ratio between the surface and the volume of the sample of 10 to 30 ml / cm2. Use a fresh solution at the start of each test. Do not change the solution even if the pH increases during the test. It is normal for the pH to increase from the initial apparent value from 0.4 to about 3 times more during the first hours depending on the amount of corrosion that occurs. Immerse the specimens in the solution using rods or supports of inert material to support the specimens above the bottom of the container. Place the test surface up in a horizontal position to prevent loss of exfoliated metal from the sample surface. Do not immerse materials containing less than 0.25% copper with those having a higher amount of copper in the same containers at the same time. After exposure and prior to mechanical testing, the specimens received cleaning according to ASTM G1-03 [13] (10 min in HNO3, acetone rinsing, drying in warm air). A uniaxial static test, to reveal the degradation of the basic mechanical properties of the material, namely yield stress, ultimate tensile strength and elongation for different aluminum alloys was performed.

3. Results and Discussion

3.1. Mechanical properties

The aim of this tensile test is to examine the influence of exfoliation corrosion for the different grades on the behavior law, which will then lead us to contribute to a better knowledge of the corrosion processes of the two aluminum alloys by studying systematically their mechanical and microstructural properties. Table 2 includes the main mechanical properties for the as-received and pre-corroded materials.

Table 2 Tensile strength properties of different aluminum alloys.

	Materials	R_e (MPa)	R_m (MPa)	K (MPa)	n
As received (un-corroded)	5083 H22	190	328	578	0.15
	2024 T3	320	485	1257	0.22
Pre-corroded	5083 H22	179	254	492	0.14
	2024 T3	202	250	1134	0.19

For the as received, the difference noted between the AA2024-T3 and the AA5083-H22 grade is explained by the fact that the first alloy belongs to the second group representing the alloys whose mechanical properties are determined by heat treatment or precipitation hardening, generally carried out at the end of the transformation process. The hardening phenomenon results from the induced and controlled precipitation of certain phases inside the aluminum matrix which will produce an increase in the mechanical properties. On the other hand, grade 5083-H22 belongs to the first group of strain hardening alloys whose mechanical properties are determined by the plastic hardening which corresponds to a structural modification of the metal, which is therefore weaker [14].

To clarify the difference between the mechanical properties of the as-received materials and the residual properties after the corrosion attack, the following figures show a comparison of these properties, namely the yield strength (Re), the tensile strength (Rm) and elongation (A%).

From Figure 2 (a), (b) and (c), we clearly see that the yield strength, ultimate strength and elongation of the materials attacked by exfoliating corrosion are reduced compared to the un-corroded metal. Therefore, the damage of these materials by this type of corrosion results in a decrease of the mechanical properties.

We notice that the materials lose in a dramatic way the ductility after the corrosion attack. The degradation of the recorded ductility is in agreement with the existence of a phenomenon controlled by volumetric diffusion [15]. Thus, Pantelakis et al. [15] have observed that sub-surface

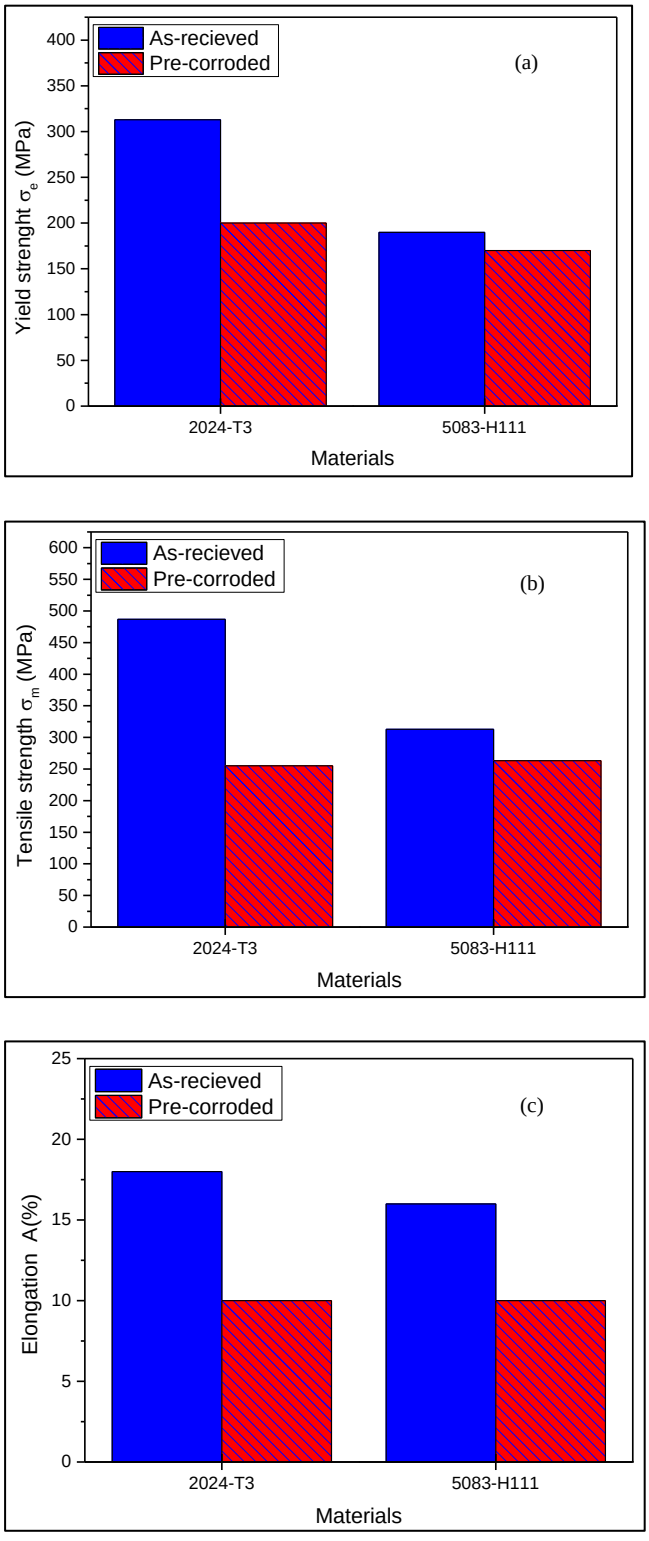

Fig. 2. Residual strength properties (a) yield strength Re, (b) tensile strength Rm and (c) Elongation A% for the different materials.

hydrogen production during exfoliating corrosion increases with exposure time. The loss of ductility is explained by the fact that there is a link between the amounts of hydrogen produced which increases very rapidly and the surface available for the penetration of this element associated with corrosion phenomena. Hydrogen is initially absorbed chemically. The increase in the density of attack sites with the exposure time in an aggressive environment tends to justify the absorption of hydrogen and its volume penetration and to highlight the link between hydrogen embrittlement and exfoliating corrosion.

The decrease of the properties of yield strength and tensile strength for the different materials returns to the surface condition affected by corrosion by introducing pitting corrosion and leaf exfoliation defects. The presence of these defects will degrade these mechanical properties by reducing its ability to withstand the load (the corroded area is no longer a bearing area) and by the concentration of stresses at the level of corrosion defects.

It is clear that the variation in the tensile strength was greater than the variation in the yield strength for the two grades of aluminum alloy. So, tensile strength is a more sensitive parameter to exfoliating corrosion.

3.2. SEM microstructural and EDS analysis

The results of the mechanical characterization tests obtained are confirmed by the microscopic analysis of the truncated and polished samples using SEM. After qualitative analysis on the 5083-H22 alloy, Figure 3 (a) shows the presence of the two elements Al and Mg with the exclusion of any other element detectable at the sensitivity threshold of the method.

Several zones, marked with a yellow circle, in this micrograph (Fig. 3c and d) were analyzed by EDS to estimate the types of intermetallics existing in these locations. The relative atomic contents in the different zones clearly demonstrate that large particles in the central part of the first micrograph (6a) are enriched magnesium and for the other (3b) that are enriched in Cu and Mg.

Based on the analysis of the zones of different contrasts it can be concluded that: The impurity elements which give the course of solidification of Al_3Mg_2 compounds near the grain boundary. These compounds do not improve the tensile strength due to their breaks and their decohesions with the matrix, providing a low resistance level when the local deformation exceeds a critical value. These results can be compared with the data recorded on the phase diagram of the alloy, which demonstrates that the results are very realistic.

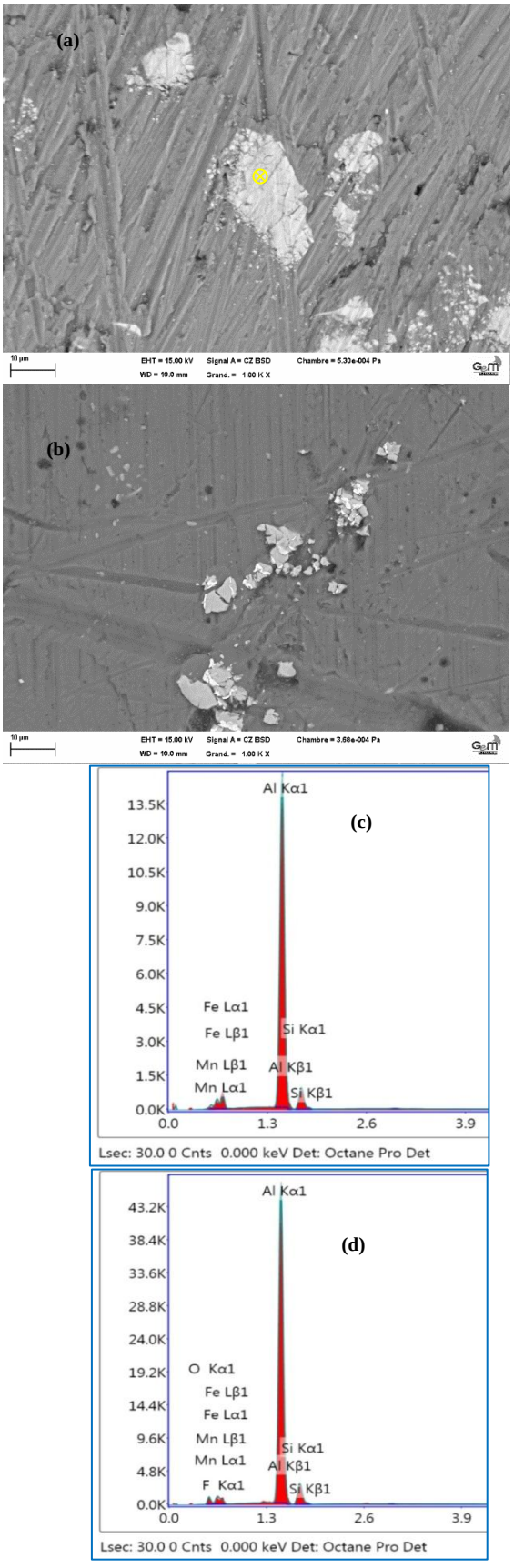

Fig. 3. SEM photomicrographs and EDX spectra showing the microstructure of : a) AA5083-H111, b) AA2024-T3 before the chemical attack.

3.2. Exfoliation corrosion

EXCO of these alloys first appears as pitting. With increasing exposure time, the pits become deeper, and a network of intergranular corrosion IGC paths starts to develop. This process of pit-to-pit interactions leads to pit clustering and coalescence. Subsequently, corrosion does not penetrate much deeper but instead spreads beneath the surface and causes exfoliation of surface layers [16].

The evolution of the degree of corrosion during a corrosion test is the first index to estimate the evolution of the severity and the degradation during the immersion. Several remarks were noted during the immersion of the specimens and samples in the solution over a period of 48 hours.

We noticed that after 4 hours of immersion there is an appearance of bubbles on both grades and that means that there is a reaction between the alumina layer and the oxygen. After 8 hours of exposure, an increase in the appearance of the bubbles was noticed with a change of color of the liquid, and after 24 hours of exposure for AA5083 and 40 hours for AA2024, a complete corrosion and intermetallic particles in the bottom of the container were noticed.

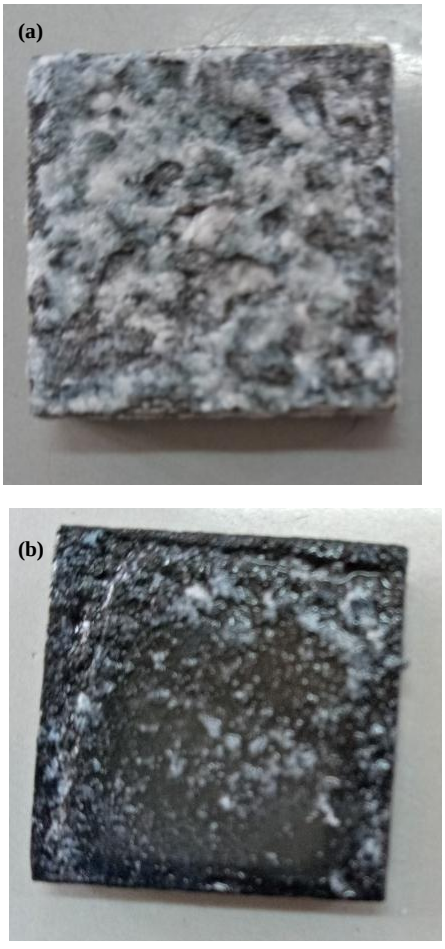

Fig.4. Degree of severity of corrosion for: a) 5083-H111, b) 2024-T3.

From figure 4, it can be seen that for both samples there is severe exfoliation corrosion with an ED performance rating. Also, a considerable massive loss was remarked for both alloys.

The morphology of the alloys was studied by SEM observation after chemical etching of the surface. These observations were made to justify the mechanical properties already found.

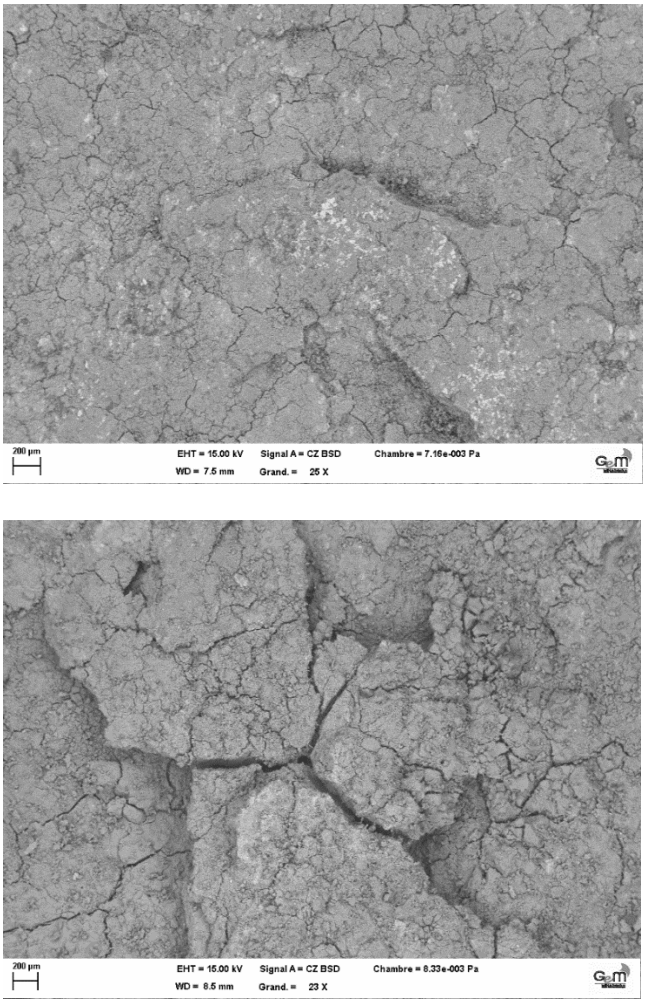

Fig. 5. SEM photomicrograph after immersion in EXCO solution for different alloys.

In Figure 5, the optical micrographs of the surfaces of the two materials after different times of immersion in the etching solution are presented. Unlike the SEM photomicrographs of Figure 3, the surfaces are very degraded and the attack is widespread, which highlights a depassivation of materials, produced by the chemical dissolution of the passive film due to alkalization of the environment.

For AA5083-H22, nitric acid dissolves the secondary phase, aluminum-magnesium intermetallic compound

(βAl-Mg). When this compound is precipitated in a relatively continuous network along the grain boundaries, the effect of the preferential attack is to corrode around the grains, which makes them fall from samples. That kind of drop of grain causes relatively large massive losses. When the compound Al_3Mg_2 is distributed in a random manner, in the case of our material figure 3a, the preferential attack can lead to intermediate-mass losses. The metallographic examination that was made reveals that the loss of mass is due to the removal of layers caused by exfoliation corrosion, which will then disturb the behavior of the material, so it will decrease the mechanical properties.

For AA2024-T3, visible separation of the metal into continuous layers and surface more degraded have been noticed and illustrated in Figure 5. The photos reveal a strong attack on mixed intermetallic particles. In these precipitates a selective dissolution of a part of the particle is observed. These zones are anodic in relation with the matrix and the rest of the same particle. It can be deduced that the noble phases of the particle must have a corrosion potential close to that of the matrix, because these (noble phases and matrix) are not attacked. After the dissolution of the intermetallic particles at the surface under the effect of the galvanic coupling [17], the passive film of the matrix controls the corrosion process of AA2024.

4. Conclusion

The main objective of this work was a comparative study of the behavior over the exfoliation corrosion of two aluminum alloys: AA2024-T3 and AA5083-H22 in EXCO solution. The main conclusions drawn from the study are:

- ✓ The 2024 T3 and 5083 H22 aluminum alloys have very different mechanical and microstructural characteristics. For AA 5083, the precipitation is less complex than for AA2024 with a type of coarse intermetallic precipitate (Al_2Mg_3) heterogeneously distributed in the Al matrix. The AA2024 exhibits more varied and complex precipitation with finer intermetallic precipitates (Al_2CuMg and Al-Cu-Mn-Fe).
- ✓ AA2024 showed higher corrosion resistance and better passivation more than AA5083. This conclusion is supported by the presence of dispersing intermetallic particles with relatively very fine grains. In addition, the EXCO test did not reveal pitting corrosion and typical exfoliation of surface layers, but rather IGC corrosion.
- ✓ EFC susceptibility was found to depend on grain size and shape as well as grain boundary composition.
- ✓ Exfoliation corrosion is a particular kind of intergranular corrosion, which is observed on the surface of the wrought materials.

References

1. Brahami A, Fajoui J, Bouchouicha B. Exfoliation Corrosion Impact on Microstructure, Mechanical Properties, and Fatigue Crack Growth of Aeronautical Aluminum Alloy. *Journal of Failure Analysis and Prevention*. 2020;20(1):197-207. https://doi.org/10.1007/s11668-020-00815-y
2. Summerson TJ, Sprowls DO. Corrosion Behavior of Aluminum Alloys, in International Conference in Celebration of the Centennial of the Hall-Heroult Process. 1986. University of Virginia, Charlottes ville, Virginia.
3. Chen Y, Liu C, Zhou J, Wang X. Multiaxial fatigue behaviors of 2024-T4 aluminum alloy under different corrosion conditions. *International Journal of Fatigue*. 2017;98:269-278.
4. Liddiard EAG, Whittaker JA, Farmery HK. *Journal of the Institute of Metals*, 89, 377-384 (1960-1961).
5. Zahavi J, Yahalom J. Exfoliation corrosion of AlMgSi alloys in water. *Journal of the Electrochemical Society*. 1982;129(6):1181.
6. Conor PC, James AD, Collier RN. Evaluation of Exfoliation Corrosion Damage to 7075-T6 Aluminum Alloy Aircraft Structural Components. Materials and Structures Group, Defense Technology Agency. 2004.
7. Sprowls DO, Walsh JD, Shumaker MB. Simplified exfoliation testing of aluminum alloys. InLocalized Corrosion—Cause of Metal Failure 1972 Jan. ASTM International.38-65.
8. Robinson MJ, Jackson NC. Exfoliation corrosion of high strength Al-Cu-Mg alloys: effect of grain structure. Corrosion Engineering, Science, and Technology. 1999;34(1):45-49.
9. Robinson MJ. Mathematical modelling of exfoliation corrosion in high strength aluminium alloys. *Corrosion Science*. 1982;22(8):775-790.
10. Kelly DJ, Robinson MJ. Influence of heat treatment and grain shape on exfoliation corrosion of Al-Li alloy 8090. *Corrosion*. 1993;49(10):787-795.
11. Standard A. G34-01: Standard Test Method for Exfoliation Corrosion Susceptibility in 2XXX and 7XXX Series Al Alloys. ASTM International: West Conshohocken, PA, USA. 2001.
12. ASTM Standard E8-04, Standard Test Methods for Tension Testing of Metallic Materials [Metric], Part 03.01, Metals Mechanical Testing Elevated and Low-Temperature Tests Metallographic.
13. American Society for Testing and Materials (Filadelfia, Pennsylvania). ASTM G1-03: Standard Practice for Preparing, Cleaning, and Evaluating Corrosion Test Specimens. ASTM. 2004.

14. Brahami A, Bouchouicha B, Zemri M, Fajoui J. Fatigue crack growth rate, microstructure and mechanical properties of diverse range of aluminum alloy: a comparison. *Mechanics and Mechanical Engineering*. 2018;22(1):329-339.
15. Pantelakis SG, Daglaras PG, Apostolopoulos CA. Tensile and energy density properties of 2024, 6013, 8090 and 2091 aircraft aluminum alloy after corrosion exposure. *Theoretical and Applied Fracture Mechanics*. 2000;33(2):117-34.
16. Kamoutsi H, Haidemenopoulos GN, Bontozoglou V, Pantelakis S. Corrosion-induced hydrogen embrittlement in aluminum alloy 2024. *Corrosion Science*. 2006;48(5):1209-1224.
17. Andreatta F, Terryn H, De Wit JH. Effect of solution heat treatment on galvanic coupling between intermetallics and matrix in AA7075-T6. *Corrosion Science*. 2003;45(8):1733-1746.

Recommended Citation

Brahami A, Fajoui J, Bouchouicha B. Experimental study of exfoliation corrosion-induced mechanical properties degradation of aluminum alloys: 2024-T3 and 5083-H22. *Alg. J. Eng. Tech.* 2020;02:022-028. http://dx.doi.org/10.5281/zenodo.3924714